Evaluation of Lower Leg Muscle Activities During Human Walking Assisted by an Ankle Exoskeleton

Wei Wang, Jianyu Chen, Yandong Ji, Wei Jin, Jingtai Liu, *Member, IEEE*, and Juanjuan Zhang

***Abstract*—Wearable robots like ankle exoskeletons have demonstrated the capability to enhance human mobility and to reduce biological efforts of human locomotion. The type of assistance provided by ankle exoskeletons could influence the lower leg muscle activities during human walking. This article aimed to systematically evaluate the lower leg muscle activities under different ankle exoskeleton assistance conditions. We measured multiple electromyography-based metrics of five lower leg muscles, while the participants walked with an ankle exoskeleton on a treadmill. Nine assistance conditions, which combined three peak times (46%, 49%, and 52% of stride time) and three peak torque levels (0.3, 0.5, and 0.7 N·m·kg^{-1}), are applied to assist plantarflexion during ankle push-off. Nine healthy subjects participated in the experiments. Of all investigated muscles, the activity level of l.SOL is influenced the most when exoskeleton assistance is applied. The root mean square of l.SOL activity reduces by 33.6 $\pm$ 14.0% under one assistance condition compared to walking without the exoskeleton. Our results can be used to guide studies on mechanical and control designs to improve neuromuscular interactions between exoskeletons and wearers.**

***Index Terms*—Ankle exoskeleton, electromyography (EMG), gait assistance, muscle activity, plantarflexion, wearable robots.**

I. Introduction

In THE past few decades, many exoskeletons have been designed to enhance human locomotion performance and to assist motion rehabilitation [1]–[3]. A fairly small number of these devices could reduce biological efforts of walking, running, or climbing stairs with predefined assistance patterns [4]–[6]. Recent advances in human-in-the-loop (HIL) optimization have demonstrated great potential to improve wearable assistive robotics performance [7]–[10]. It uses real-time measurements of human physiological signals as optimization objectives to continuously update exoskeleton control parameters and thus to generate customized assistance patterns. In this process, subjects experience a wide range of assistance conditions.

In previous studies, metabolic cost was widely used as the HIL optimization objective of exoskeleton assistance conditions. Multiple studies have discussed the metabolic cost of human beings during exoskeleton-assisted walking [4], [5], [11]–[16]. They found that when appropriate exoskeleton assistance patterns were applied, the metabolic rate of the human body could be reduced during walking. The metabolic rate has been commonly used as a physiological indicator for the effectiveness of various exoskeleton assistance patterns, and thus, it often serves as the objective of HIL optimization [7]–[9]. However, measuring of metabolic cost, which is usually through an indirect calorimetry, is noisy, delayed, and sparsely sampled. These characteristics lead to long evaluation times and, thus, an inefficient optimization process. For example, one study optimized four lower limb exoskeleton control parameters based on metabolic cost within 64-min walking [8]. Another one optimized two parameters in an average of 21.4 $\pm$ 1.0 min [9]. Meanwhile, both indirect calorimetry equipment and nonoptimized exoskeletons are uncomfortable to wear and may induce faster human fatigue. This results in unpleasant experimental experiences and inaccurate experimental outcomes. Therefore, there have been motivations to explore the possibility of using other physiological responses as HIL optimization objectives. One such reasonable candidate is muscle activity. Currently, the effectiveness of muscle activity levels being used as optimization objectives has not been thoroughly evaluated. A key measurement method for muscle activity intensity is the surface electromyography (sEMG). Electromyography (EMG) signals contain important information about energy consumption of muscle contractions and have been widely used to control wearable robotic devices and to evaluate their effects on human performance [17]–[20]. It is necessary and important to systematically evaluate relevant muscle activities in different ankle exoskeleton assistance conditions to provide comprehensive understanding about the

Manuscript received September 15, 2019; revised December 21, 2019; accepted January 23, 2020. Date of publication February 17, 2020; date of current version July 29, 2020. This work was supported in part by the National Key Research and Development Program of China under Grant 2017YFB1303005, in part by the National Natural Science Foundation of China under Grant 61703214, in part by the Natural Science Foundation of China under Grant 91848108, and in part by the National Natural Science Foundation of Tianjin under Grant 17JCYBJC40600. Paper no. TII-19-4246. *(Corresponding author: Juanjuan Zhang.)*

The authors are with the Tianjin Key Laboratory of Intelligent Robotics, Institute of Robotics and Automatic Information Systems, Nankai University, Tianjin 300350, China (e-mail: nk_wangwei@mail.nankai.edu.cn; jychen@mail.nankai.edu.cn; jiyandong0204@outlook.com; 1960516506@qq.com; liujt@nankai.edu.cn; juanjuanzhang@nankai.edu.cn).

Color versions of one or more of the figures in this article are available online at http://ieeexplore.ieee.org.

Digital Object Identifier 10.1109/TII.2020.2974232

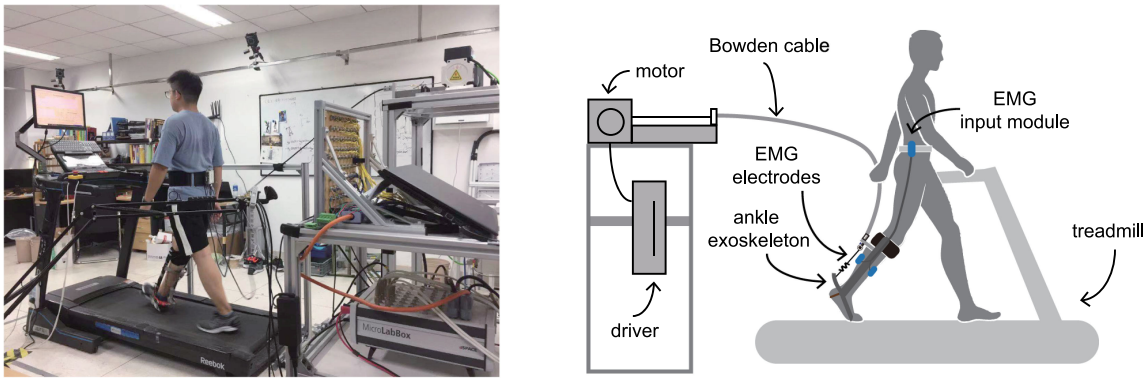

Fig. 1. Ankle exoskeleton experimental platform. (a) Photograph of the experimental setup. (b) Schematic diagram of the experimental setup. Subjects walked on a treadmill while wearing an ankle exoskeleton on the right ankle joint. The ankle plantarflexion assistive torque generated from a motor and transmitted to the ankle exoskeleton through a flexible Bowden cable. EMG electrodes were placed on the right lower leg to measure muscle activities.

mechanism of human walking assisted by an ankle exoskeleton. It is also important to verify the effectiveness of using muscle activities in HIL optimization.

Our goal was to systematically investigate the influence of assistance conditions on lower leg muscle activities while human walking with an ankle exoskeleton. We focused mainly on lower leg muscles, which were closer to the assisted human joint and have been shown to be more affected during exoskeleton-assisted human walking [12], [21], [22]. We used a unilateral ankle exoskeleton to assist plantarflexion movements during human walking and changed assistive torque profiles in a broad range to study the influence of different exoskeleton assistance patterns on the exoskeleton-side lower leg muscle activities of walking. We expected our study to help to evaluate exoskeleton performance and develop advanced control algorithms based on EMG. Furthermore, results of this study could help to guide the selection of the HIL optimization objective.

II. Methods

We investigated the lower leg muscle activities on a tethered unilateral ankle plantarflexion assistance exoskeleton testbed. All subjects walked on a treadmill under a fixed speed while wearing the exoskeleton on the right foot. The assistive torque was enforced with a combination of proportional–derivative control and iterative learning control. We applied nine different assistive torque profiles, each defined by a unique combination of peak time and peak torque values, and collected the corresponding EMG measurements of five lower leg muscles. We calculated three metrics from the raw EMG signals and performed statistical analysis on them among various walking conditions.

A. Ankle Exoskeleton Experimental Platform

We built an ankle exoskeleton-assisted human walking experimental platform (see Fig. 1) [8], [25]. It consisted of an ankle exoskeleton that interfaces with the human shank and foot, a high-speed control system responsible for torque control, multiple sensors, and an offboard actuation system that generated and transmitted assistive torque to the exoskeleton [8], [23]–[25]. The hardware configuration of the system is shown in Fig. 2(b).

1) Ankle Exoskeleton: The ankle exoskeleton mainly comprised of three components: a shank frame, a foot frame, and a titanium ankle lever, joined together with two joint shafts on each side of the human ankle [see Fig. 2(a)] [25]. Assistive torque was transmitted to the titanium lever through a Bowden cable. The cable was threaded with a pulley and connected with a series spring, which increased the passive compliance of human exoskeleton interactions [26]. A heel rope was placed in the bottom of a shoe that was used to lift the heel when assistive torque was provided.

2) Control System: A real-time controller (DS1202, dSPACE, Paderborn, GmbH) was used to sample measured data from sensors and to generate motor velocity commands. Motor velocity commands were generated at a frequency of 500 Hz.

3) Sensors: sEMG signals were measured by a wired EMG system (Bagnoli, Delsys, Natick, MA, USA). The assistive torque was measured by a Wheatstone bridge consisting of four strain gauges (KFH-6-350-C1-11L1M2R, OMEGA Engineering, Norwalk, CT, USA). Strain gauge signals were then amplified by a signal conditioner (IAA100, Futek, Irvine, CA, USA). Two digital optical encoders (E5, US Digital, Vancouver, WA, USA) were installed on motor shaft and exoskeleton joint shaft, respectively, to measure the motor position and the ankle joint angle. A footswitch (McMaster-Carr, Aurora, OH, USA) was attached inside the exoskeleton shoe to detect heel strike.

4) Actuation System: The actuation system was composed of an ac brushless servo motor, a 5:1 planetary gear, and a motor driver (BSM90N-175AA, GBSM90-MRP120-5, and MF180-04AN-16 A, ABB, Zurich, Switzerland). Then, the torque generated from the motor was transmitted to the ankle exoskeleton through the flexible Bowden cable.

B. Torque Control

Assistive torque was tracked using a combination of proportional–derivative control and iterative learning algorithm (PD-LRN) [23], [24]. Iterative learning control is suitable for

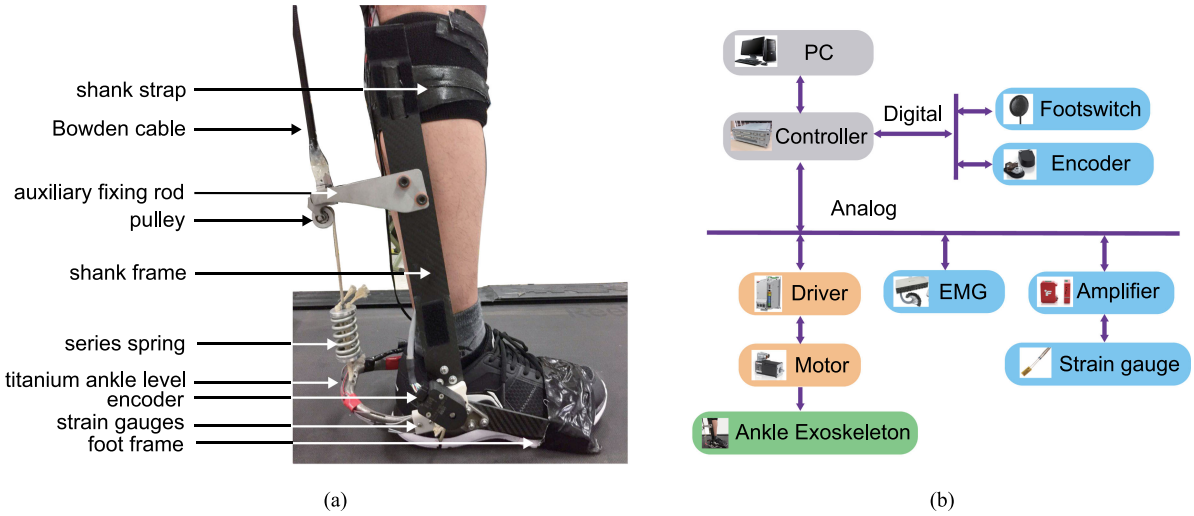

Fig. 2. Ankle exoskeleton mechanical structure and system hardware configuration. (a) Mechanical structure of the ankle exoskeleton. Shank frame, foot frame, and titanium ankle level joined together in the biological ankle joint. A Bowden cable was threaded a pulley and a series spring, and connected with the ankle level. A Wheatstone bridge consisted of four strain gauges was used to measure the assistive torque. An encoder was installed on the exoskeleton joint shaft to measure the ankle joint angle. A footswitch was attached inside the exoskeleton shoe to detect heel strike. (b) Hardware configuration of the system. The system comprised: 1) an ankle exoskeleton (green); 2) a high-speed control system (gray); 3) sensors that measure muscles EMG signals and exoskeleton performance (blue); and 4) motor and driver (orange).

systems performed the same tasks repetitively and periodically [27]. Human walking exhibits cyclic behavior. During human walking assisted by an ankle exoskeleton on a treadmill, torque error in the last gait cycle can be used to modify motor velocity for the next gait cycle. A P-type iterative learning controller was used to reduce the steady-state errors of torque tracking. The PD-LRN torque controller can be expressed by the following equation [23], [24]:

$$\begin{aligned}
\dot{\theta}_{m,\mathrm{des}}(i,n) &= \frac{1}{T}\cdot\Delta\theta_{m,\mathrm{des}}(i,n)\\
\Delta\theta_{m,\mathrm{des}}(i,n) &= -K_P\cdot e_\tau(i,n) - K_D\cdot\dot{\theta}_m(i,n)\\
&\quad + \Delta\theta^{\mathrm{LRN}}_{m,\mathrm{des}}(i+D,n)\\
\Delta\theta^{\mathrm{LRN}}_{m,\mathrm{des}}(i,n+1) &= \beta\cdot\theta^{\mathrm{LRN}}_{m,\mathrm{des}}(i,n) - K_L\cdot e_{\mathrm{flt}}(i,n)\\
e_{\mathrm{flt}}(i,n) &= (1-K_{\mathrm{flt}})\cdot e_{\mathrm{flt}}(i,n-1)\\
&\quad + K_{\mathrm{flt}}\cdot e_\tau(i,n) \qquad (1)
\end{aligned}$$

where $\dot{\theta}_{m,\mathrm{des}}$ is the desired motor velocity, $\Delta\theta_{m,\mathrm{des}}$ is the desired motor displacement, $\dot{\theta}_m$ is the measured motor velocity, $\Delta\theta^{\mathrm{LRN}}_{m,\mathrm{des}}$ is the learned feedforward compensation from the iterative learning algorithm, and e_{flt} is a torque error filter. K_P, K_D, and K_L are proportional gain, derivative gain, and iterative learning gain, respectively. $e_\tau = \tau - \tau_{\mathrm{des}}$ is the torque error. i is the time index within a gait cycle, n is the stride number, T is a constant related to the motor rise time, and D is the estimated number of time indices for the time delay between motor velocity commands and motor rotation. The time delay was about 18 ms according to our previous tests. $K_{\mathrm{flt}} \in [0,1]$ is a weight on the learned error. $\beta \in [0,1]$ is a weighting term of the learned torque trajectory. Torque control parameters were systematically adjusted to minimize the tracking error (see Table I). The reported tracking error was as low as 1% of peak desired torque. No sensible delay or oscillation was detected by the participants [23].

TABLE I
PARAMETER VALUES OF THE PD-LRN TORQUE CONTROLLER

K_P	K_D	K_L	K_{flt}	β	D	T
2.2	0.01	0.15	1	1	0.018s	0.050s

C. Assistive Torque Profile

We defined the desired plantarflexion assistive torque profile as a single-peak curve according to human walking biomechanics [28], [29]. We used two cubic splines joined at their peaks to realize this curve [8]. Then, two parameters were used to define the assistive torque profile: peak time and peak torque [see Fig. 3(a)]. Peak time was referred to the time that ankle exoskeleton provided the maximum plantarflexion assistive torque. Peak time was normalized to percent stride and was denoted as $X\%$. Peak torque was referred to the maximum plantarflexion assistive torque that ankle exoskeleton provided for the wearer. Peak torque was normalized to body weight and was presented in unit of $\mathrm{N{\cdot}m{\cdot}kg^{-1}}$.

To compare the lower leg muscle activities of ankle exoskeleton-assisted walking, we designed nine different exoskeleton assistance conditions that combined three different peak times and three different peak torque levels [see Fig. 3(b)]. Three peak times were 46%, 49%, and 52% of a gait cycle (represented as early, middle, and late peak times). We constrained peak time to between 45% and 53% of a gait cycle because most healthy subjects ankle push-off timings were in this range [22], [28], [29]. Moreover, these three peak time values that we selected could distinguish different

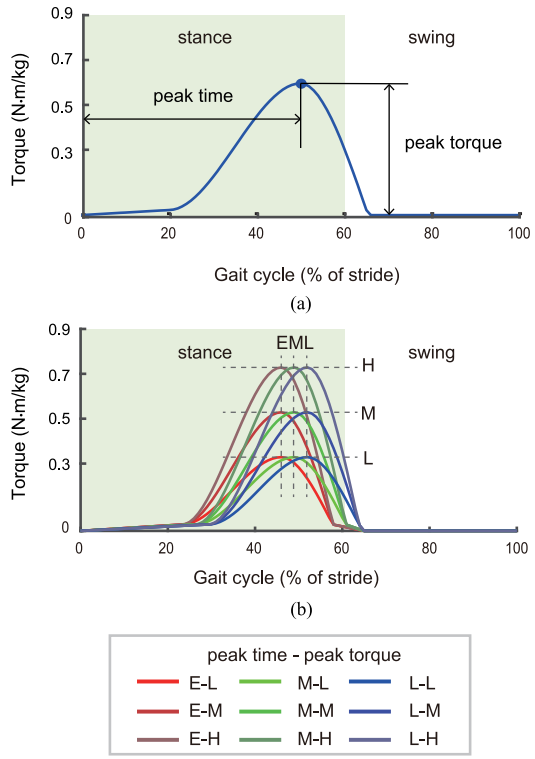

Fig. 3. Plantarflexion assistive torque profile. (a) Assistive torque profile. Peak time referred to the time that ankle exoskeleton provided the maximum ankle plantarflexion torque. Peak torque referred to the maximum assistive torque that the exoskeleton provided for the wearer. (b) Nine different exoskeleton assistance conditions that applied in the experiment. Based on the combinations of three peak times and three peak torque levels, the nine different assistance conditions were EL, EM, EH, ML, MM, MH, LL, LM, and LH. We grouped exoskeleton assistance conditions by peak time. Early, Middle, and Late peak times are marked in red, green, and blue, respectively. Darker colors refer to higher peak torque levels. The light green rectangle shows the stance phase in a gait cycle. Dash lines show the three peak times and three peak torque levels.

assistance and were to be close to the optimal peak time from a previous study [8]. Three plantarflexion peak torque levels were 0.3, 0.5, and 0.7 $N{\cdot}m{\cdot}kg^{-1}$ (represented as low, medium, and high peak torque). Peak torque was bounded within 0.3–0.7 $N{\cdot}m{\cdot}kg^{-1}$ to ensure comfortability during walking test. Too higher assistive peak torque could induce discomfort in cases with unusual timing. Too smaller assistive peak torque would be unable to provide appreciable assistance. The nine different assistance conditions were thus referred as Early-time-Low-torque (EL), Early-time-Medium-torque (EM), Early-time-High-torque (EH), Middle-time-Low-torque (ML), Middle-time-Medium-torque (MM), Middle-time-High-torque (MH), Late-time-Low-torque (LL), Late-time-Medium-torque (LM), and Late-time-High-torque (LH).

D. Participants and Experimental Protocol

Nine healthy male subjects (age 22.3 $\pm$ 3.2 years; weight 67.4 $\pm$ 9.5 kg; height 177.1 $\pm$ 4.2 cm; and mean $\pm$ S.D.) participated in the experiment. All participants were provided with written informed consent before completing the protocol, which was approved by the ethical committee of Nankai University.

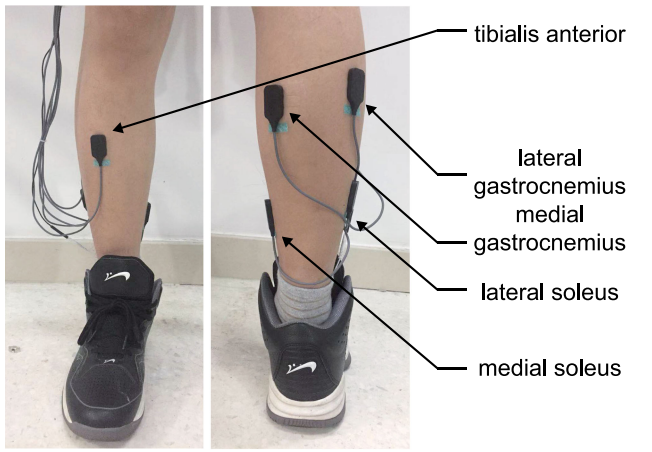

Fig. 4. EMG electrodes in the right lower leg muscles. EMG signals were measured from five lower leg muscle positions: TA, m.SOL, l.SOL, m.GAS, and l.GAS. Electrodes were fixed by medical adhesive tapes to keep in close contact with skin.

The experimental protocol included two sessions for each participant: a training session and a testing session. Participants walked on a treadmill at 1.25 $m{\cdot}s^{-1}$ while wearing the ankle exoskeleton on the right ankle joint in all sessions.

The training session was performed on the first day. All exoskeleton assistance conditions were applied to the subjects to ensure that they adapt to walking with the exoskeleton. Moreover, subjects were advised to relax lower leg muscles and not to resist the exoskeleton assistance.

The testing session was performed on a separate day, at least 48 h later to avoid fatigue-induced effects. It started with a 4-min warming-up and followed by a 2-min normal walking (NW) condition, in which participants walked without the exoskeleton. Next, subjects performed a 2-min zero-torque (ZT) condition, in which they walked with the exoskeleton applying zero assistive torque to the human ankle. Then, the nine different assistance conditions were applied in random order. To minimize the effects of adaptation and fatigue, subjects were asked to experience the nine different assistance conditions again but in a reverse order. Then, the testing session ended by subjects performing a ZT condition. All conditions lasted 2 min to ensure that muscle activities reached the steady state. Resting breaks of 2–5 min were given between all conditions according to subjects' own requests. One subject did not test the conditions in reverse order due to hardware malfunction. Another two subjects unfinished LH condition because they cannot adapt to this condition.

E. Data Collection and Analysis

We measured lower leg muscle activities using a wired EMG system. sEMG signals were measured from five right lower leg muscles: tibialis anterior (TA), medial soleus (m.SOL), lateral soleus (l.SOL), medial gastrocnemius (m.GAS), and lateral gastrocnemius (l.GAS) (see Fig. 4). These muscles are primarily responsible for human ankle plantarflexion and dorsiflexion movements in a sagittal plane. Electrodes were placed according to the guidance in [30]. Sampling frequency was set to 5000 Hz. Raw EMG signals were high-pass filtered with a second-order

TABLE II
PEARSON CORRELATION COEFFICIENTS ACROSS DIFFERENT EMG METRICS

R	mean value	max value	RMS value
mean value	-	75.5%	90.0%
max value	75.5%	-	95.4%
RMS value	90.0%	95.4%	-

Butterworth filter (cutoff frequency 20 Hz), full-wave rectified, and low-pass filtered with a second-order Butterworth filter (cutoff frequency 10 Hz). All preprocessed EMG amplitudes were then normalized to the average EMG peak value during the last minute of the NW session for the same participants.

Three EMG-based metrics in the time domain were calculated to quantify changes of muscle activities during exoskeleton-assisted walking: the root-mean-square (rms) value, the mean value, and the peak value of the measured lower leg muscle EMG over a whole stride [31], [32]. EMG metrics for each condition were calculated from the last minute of corresponding walking data. Pearson correlation coefficients were calculated to evaluate the correlation between all EMG metrics.

F. Statistical Analysis

Repeated measure analyses of variance (ANOVA), including ten conditions (NW, EL, ML, LL, EM, MM, LM, EH, MH, and LH), was conducted to verify the effects of plantarflexion assistance on lower leg muscle activities compared to the NW condition. Then, repeated measure ANOVA, including ten conditions (ZT, EL, ML, LL, EM, MM, LM, EH, MH, and LH), was conducted to identify differences in muscle activities between all assistance conditions and the ZT condition. The significance level was set at $\alpha = 0.05$. Statistical analyses were conducted with MATLAB (MathWorks, Natick, MA, USA). We also performed student's paired *t*-test to compare rms of l.SOL muscle activity of nine exoskeleton assistance conditions with each other.

III. RESULTS

Table II shows the Pearson correlation coefficients between all EMG metrics. Lower leg muscle EMG RMS values were well corrected with both mean and max values, with correlation coefficients being 90.0% and 95.4%, respectively. Therefore, muscle activity rms values were selected as the primary metric to be investigated.

Exoskeleton-side lower leg muscle activities over the whole stride in different walking conditions are shown in Fig. 5. RMS values of these muscle activities in different walking conditions are shown in Table III. Fig. 6 shows the changes of l.SOL activity in different exoskeleton assistance conditions with respect to NW and ZT conditions.

The l.SOL muscle activity, particularly in stance phase, was reduced most significantly during human walking assisted by the ankle exoskeleton (see Figs. 5(a) and 6, Table III). Under one specific assistance condition, middle peak time, and high peak torque (MH), the rms of l.SOL muscle activity was 0.195 $\pm$ 0.042. This means a reduction of 33.6 $\pm$ 14.0% compared to the NW condition ($P < 0.05$), and a reduction of 24.9 $\pm$ 19.5% compared to the ZT condition ($P < 0.05$). Fairly large differences in rms of l.SOL muscle activity were found under this condition with respect to other six assistance conditions (EL, $P = 5.5 \times 10^{-3}$; EM, $P = 1.5 \times 10^{-2}$; EH, $P = 1.3 \times 10^{-3}$; ML, $P = 4.3 \times 10^{-3}$; MM, $P = 7.0 \times 10^{-3}$; and LL, $P = 1.8 \times 10^{-2}$). No significant differences were found between MH and other two assistance conditions (LM, $P = 0.066$; LH, $P = 0.73$). Furthermore, under LH and MM assistance conditions, the rms value of l.SOL activity significantly decreased compared to walking with the exoskeleton but provide zero assistive torque ($P = 3.7 \times 10^{-2}$ and $P = 9.0 \times 10^{-3}$; see Fig. 6).

There were no significant differences in the TA muscle activity between exoskeleton assistance conditions and the NW condition [$P = 0.71$; see Fig. 5(a), Table III]. For the m.SOL, changes of muscle activity under different assistance conditions were not obvious compared to the NW condition [$P = 0.96$; see Fig. 5(a), Table III]. For the m.GAS and l.GAS, changes of muscle activities were not obvious compared to the NW condition [$P = 1.0$ and $P = 1.0$; see Fig. 5(a), Table III]. There were no significant changes of these muscle activities under exoskeleton-assisted walking conditions compared to the ZT condition (Table III).

IV. DISCUSSION

The aim of this research was to evaluate lower leg muscle activities during human walking assisted by an ankle exoskeleton. In our experiments, the assistive torque was applied accurately to the wearers by using a PD-LRN control algorithm. We designed nine exoskeleton assistance conditions to evaluate lower leg muscle activity changes. Meanwhile, the RMS values of the measured EMG signals from right lower leg were used as an indicator of the EMG-based metric.

The l.SOL muscle activity showed the biggest differences among different walking conditions. It had decreased activities under all assistance conditions compared to NW and ZT conditions. Meanwhile, the reductions of l.SOL activity varied among different assistance conditions. This result indicates that ankle exoskeleton assistance has a positive effect on l.SOL and also suggests that the l.SOL muscle activity is suitable for being selected as a candidate objective of HIL optimization. The significant reductions of the l.SOL muscle activity during exoskeleton assistance can be explained from biomechanics. The soleus muscle connects calf and phalanges and has a higher proportion of slow muscle fibers. Soleus muscle contractions complete the primary plantarflexion movements during human walking [33]. Therefore, when plantarflexion assistive torque was applied to the wearer through the exoskeleton, the soleus muscle contractions were partially replaced by the exoskeleton assistance and led to soleus muscle activity reductions. This explanation also suggests that the assistive torque that our ankle exoskeleton provided was consistent with human walking biomechanics.

Changes of other lower leg muscles during ankle exoskeleton-assisted walking were not significant. The TA muscle activity had no obvious changes when assisted by low and medium

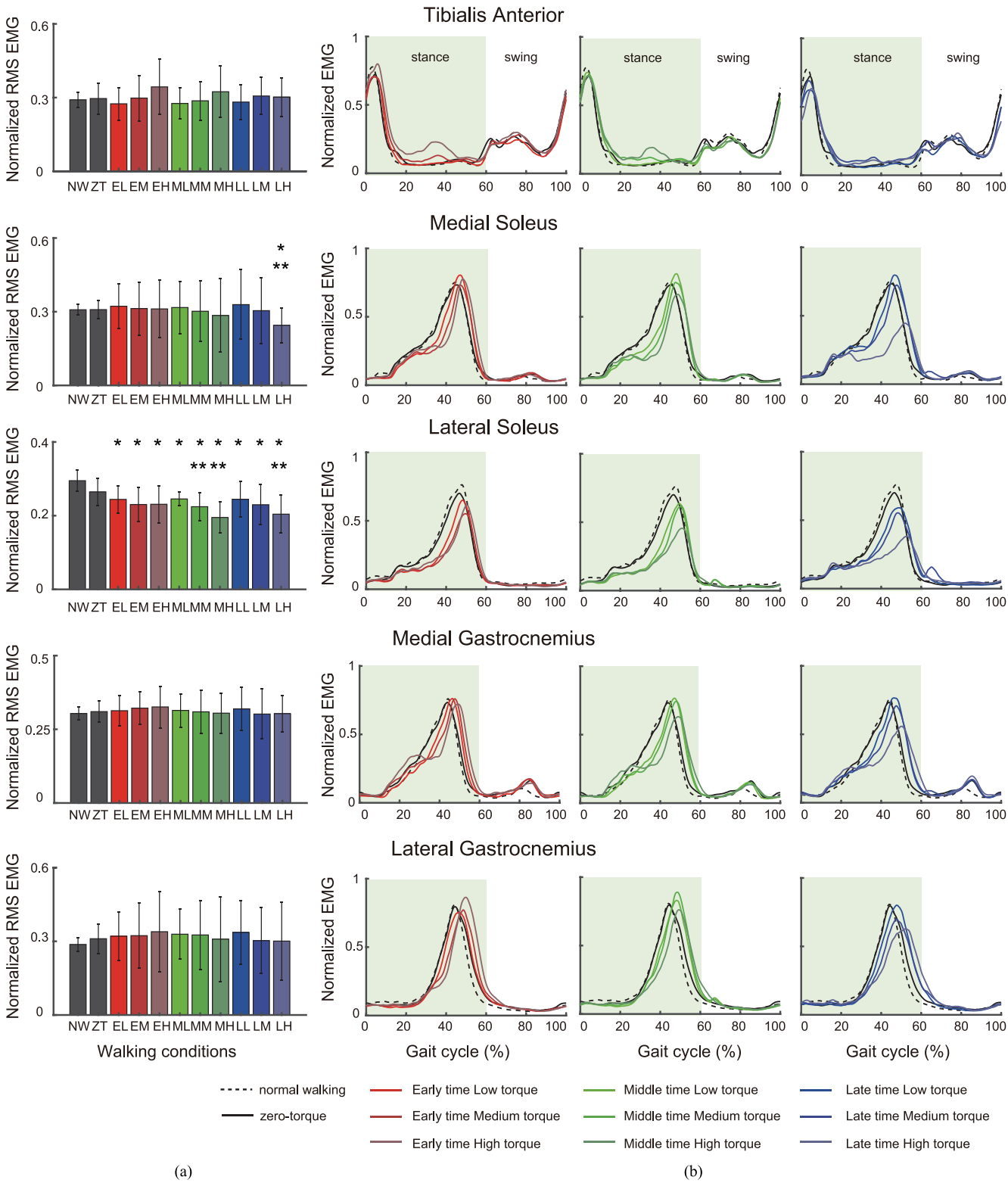

Fig. 5. Lower leg muscle activities over the whole stride in different exoskeleton assistance conditions. (a) RMS normalized stride-wise EMG from $N = 9$ subjects. Bars and whiskers are subject means and standard deviations of the whole stride RMS average muscle activity. * represents statistically significant differences with respect to the NW condition. ** represents statistically significant differences with respect to the ZT condition. (b) Lower leg muscle activities (TA, m.SOL, l.SOL, m.GAS, and l.GAS) over the stride from one side heel contact (0% of a gait cycle) to opposite side toe off (100% of a gait cycle) in human walking in different ankle exoskeleton assistance conditions. We grouped exoskeleton assistance conditions by peak time. Early, Middle, and Late peak times are marked in red, green, and blue, respectively. Darker colors refer to higher peak torque levels. The light green rectangle shows the stance phase in a gait cycle.

TABLE III
RMS OF LOWER LEG MUSCLE ACTIVITIES DURING DIFFERENT WALKING CONDITIONS

Peak Time (% of stride)	Peak Torque ($N \cdot m \cdot kg^{-1}$)	RMS				
		TA	m.SOL	l.SOL	m.GAS	l.GAS
46	0.3	0.274±0.066	0.322±0.092	0.244±0.037*	0.313±0.051	0.321±0.10
	0.5	0.298±0.093	0.313±0.108	0.230±0.047*	0.322±0.055	0.323±0.132
	0.7	0.344±0.113	0.311±0.118	0.231±0.051*	0.326±0.071	0.339±0.165
49	0.3	0.276±0.062	0.317±0.106	0.245±0.019*	0.314±0.056	0.329±0.101
	0.5	0.287±0.079	0.302±0.123	0.224±0.038*,**	0.309±0.073	0.326±0.140
	0.7	0.324±0.104	0.285±0.149	0.195±0.042*,**	0.305±0.068	0.309±0.172
52	0.3	0.282±0.071	0.329±0.142	0.245±0.049*	0.319±0.073	0.336±0.130
	0.5	0.307±0.075	0.304±0.134	0.230±0.054*	0.302±0.085	0.303±0.134
	0.7	0.302±0.079	0.245±0.071*,**	0.204±0.051*,**	0.303±0.062	0.301±0.158
normal walking		0.291±0.031	0.308±0.022	0.295±0.028	0.304±0.022	0.287±0.029
zero-torque		0.296±0.063	0.309±0.037	0.265±0.037	0.310±0.036	0.311±0.060

* statistically significant differences with respect to the NW condition.
** statistically significant differences with respect to the ZT condition.
TA, tibialis anterior; m.SOL, medial soleus; l.SOL, lateral soleus; m.GAS, medial gastrocnemius; l.GAS, lateral gastrocnemius.

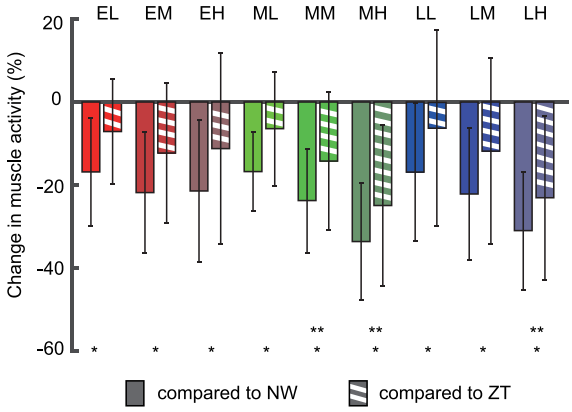

Fig. 6. Changes of l.SOL activity in different exoskeleton assistance conditions with respect to NW and ZT conditions. Muscle activity was quantified as the RMS of the processed EMG signals. Bars and whiskers are subject means and standard deviations of the whole stride RMS average l.SOL muscle activity. Solid bars and striped bars indicate change of muscle activity in exoskeleton assistance conditions compared to NW and ZT conditions. We grouped exoskeleton assistance conditions by peak time. Early, Middle, and Late peak times are marked in red, green, and blue, respectively. Darker colors refer to higher peak torque levels. * represents statistically significant differences with respect to the NW condition. ** represents statistically significant differences with respect to the ZT condition.

peak torque. However, muscle activity increased when high peak torque was applied, especially at early and middle peak time [see Fig. 5(b)]. This may be due to the coactivation of TA to counteract inappropriate exoskeleton assistive torque. From biomechanics, TA acts antagonistically to the exoskeleton, which means high peak torque may negatively influence the muscle activity. This also suggests that TA can be used as a balance term in the HIL optimization objective, and preferable assistance seems to be a tradeoff between more l.SOL activity reductions and less TA activity increases. For the m.SOL, except under the LH condition, muscle activity had no statistically significant differences with respect to the NW condition or the ZT condition. The same as l.SOL, m.SOL activity significantly decreased under the LH condition compared to NW and ZT conditions ($P < 0.05$ and $P < 0.05$) Table III. This suggests that assistance with late peak time and high peak torque may further decrease lower leg muscle activities during exoskeleton-assisted walking. The m.GAS and l.GAS muscle activities under all exoskeleton assistance conditions were not significantly changed compared to NW and ZT conditions. Peak EMG changes were not observed compared to the NW condition [see Fig. 5(b)]. From biomechanics aspects, the gastrocnemius has higher proportion of fast muscle fibers and is primarily involved in movements like running and jumping that need to provide greater muscle contraction force in a short period of time. However, the gastrocnemius is less involved in walking and standing. This explanation suggests that the gastrocnemius may not be a good choice for evaluating ankle exoskeleton assistance performance. Moreover, for our ankle exoskeleton, the shank strap of the ankle exoskeleton is close to the gastrocnemius. This may affect gastrocnemius contraction and increased measuring noise of EMG signals around strap.

We also analyzed the effects of peak time and peak torque on l.SOL activity independently. There were no significant differences in l.SOL activity between early, middle, and late peak time assistance conditions. For example, under EM, MM, and LM conditions, the RMS values of l.SOL activity have no obvious changes. This suggests that the peak time may not be a determinant factor of the exoskeleton assistance that can influence l.SOL activity. However, significant differences were found in l.SOL activity between low, medium, and high peak torque assistance conditions ($P < 0.05$). As shown in Fig. 6, higher peak torque could reduce more l.SOL activity. This indicates that exoskeleton assistive peak torque levels can greatly affect l.SOL activity. This is also consistent with our expectations that human biological efforts like muscle activity will decrease as the assistive torque levels increases.

It is worth noting that our experiments have limitations. One is that the participants we currently recruited were almost young people. Both old subjects and disabled subjects would be recruited in future works. Another is that we conducted a small-scale test to compare metabolic cost and muscle activities under MH, EH, NW, and ZT conditions. According to the one subject data, the l.SOL activity decreased under MH and EH conditions.

Metabolic cost decreased in these two conditions compared to the ZT condition, and it increased compared to the NW condition. The relationship between muscle activities and metabolic cost under exoskeleton-assisted walking seems to be complicated. Future works would be required to recruit more subjects and to conduct more experiments to explore the relationship among metabolic cost, muscle activities, and other physiological responses under different exoskeleton assistance conditions.

V. Conclusion

In this article, we systematically evaluated lower leg muscle activities and quantified changes of EMG-based metrics during human walking assisted by an ankle exoskeleton. The l.SOL muscle activity showed significant reductions when exoskeleton assistance was applied, and it was most reduced under one of the nine conditions. The l.SOL muscle activity has the potential to be used as a candidate objective of HIL optimization. In future works, we plan to recruit subjects with different ages and to conduct experiments to compare the relationship between muscle activities and other physiological responses during different exoskeleton assistance conditions.

Acknowledgment

The authors would like to thank H. Han, X. Li, and S. Zhang for assistance with data collection and suggestions for improving this article. The authors would also like to thank all the participants who gave their time for this article.

References

[1] W. Cornwall, "In pursuit of the perfect power suit," *Science*, vol. 350, no. 6258, pp. 270–273, 2015.
[2] A. M. Dollar and H. Herr, "Lower extremity exoskeletons and active orthoses: Challenges and state-of-the-art," *IEEE Trans. Robot.*, vol. 24, no. 1, pp. 144–158, Feb. 2008.
[3] A. J. Young and D. P. Ferris, "State of the art and future directions for lower limb robotic exoskeletons," *IEEE Trans. Neural Syst. Rehabil. Eng.*, vol. 25, no. 2, pp. 171–182, Feb. 2017.
[4] P. Malcolm, W. Derave, S. Galle, and D. D. Clercq, "A simple exoskeleton that assists plantarflexion can reduce the metabolic cost of human walking," *PLoS ONE*, vol. 8, 2013, Art. no. e56137.
[5] G. Lee *et al.*, "Reducing the metabolic cost of running with a tethered soft exosuit," *Sci. Robot.*, vol. 2, 2017, Art. no. eaan6708.
[6] M. Chandrapal, X. Chen, and W. Wang, "Preliminary evaluation of a lower-limb exoskeleton—Star climbing," in *Proc. IEEE/ASME Int. Conf. Adv. Intel. Mechatron.*, 2013, pp. 1458–1463.
[7] J. R. Koller, D. H. Gates, D. P. Ferris, and C. D. Remy, "'Body-in-the-loop' optimization of assistive robotic devices: A validation study," in *Proc. Robot.: Sci. Syst. Conf.*, 2016, doi: 10.15607/RSS.2016.XII.007.
[8] J. Zhang *et al.*, "Human-in-the-loop optimization of exoskeleton assistance during walking," *Science*, vol. 356, pp. 1280–1284, 2017.
[9] Y. Ding, M. Kim, S. Kuindersma, and C. J. Walsh, "Human-in-the-loop optimization of hip assistance with a soft exosuit during walking," *Sci. Robot.*, vol. 3, 2018, Art. no. eaar5438.
[10] L. Schiatti, J. Tessadori, N. Deshpande, G. Barresi, L. C. King, and L. S. Mattos, "Human in the loop of robot learning: EEG-based reward signal for target identification and reaching task," in *Proc. IEEE Int. Conf. Robot. Autom.*, 2018, vol. 3, pp. 4473–4480.
[11] A. Gams, T. Petric, T. Debevec, and J. Babic, "Effects of robotic knee exoskeleton on human energy expenditure," *IEEE Trans. Biomed. Eng.*, vol. 60, no. 6, pp. 1636–1644, Jun. 2013.
[12] S. Galle, P. Malcolm, S. H. Collins, and D. D. Clercq, "Reducing the metabolic cost of walking with an ankle exoskeleton: Interaction between actuation timing and power," *J. Neuroeng. Rehabil.*, vol. 14, 2017, Art. no. 35.
[13] Y. Ding *et al.*, "Effect of timing of hip extension assistance during loaded walking with a soft exosuit," *J. Neuroeng. Rehabil.*, vol. 13, 2016, Art. no. 87.
[14] P. Malcolm, R. E. Quesada, J. M. Caputo, and S. H. Collins, "The influence of push-off timing in a robotic ankle-foot prosthesis on the energetics and mechanics of walking," *J. Neuroeng. Rehabil.*, vol. 12, 2015, Art. no. 21.
[15] S. H. Collins, M. B. Wiggin, and G. S. Sawicki, "Reducing the energy cost of human walking using an unpowered exoskeleton," *Nature*, vol. 522, pp. 212–215, 2015.
[16] J. R. Koller, D. A. Jacobs, D. P. Ferris, and C. D. Remy, "Learning to walk with an adaptive gain proportional myoelectric controller for a robotic ankle exoskeleton," *J. Neuroeng. Rehabil.*, vol. 12, 2015, Art. no. 97.
[17] O. M. Blake and J. M. Wakeling, "Estimating changes in metabolic power from EMG," *Springerplus*, vol. 2, 2013, Art. no. 229.
[18] C. Fleischer and G. Hommel, "A human–exoskeleton interface utilizing electromyography," *IEEE Trans. Robot.*, vol. 24, no. 4, pp. 872–882, Aug. 2008.
[19] P. G. Jung, G. Lim, S. Kim, and K. Kong, "A wearable gesture recognition device for detecting muscular activities based on air-pressure sensors," *IEEE Trans. Ind. Informat.*, vol. 11, no. 2, pp. 485–494, Apr. 2015.
[20] Y. Zhuang, S. Yao, C. Ma, and R. Song, "Admittance control based on EMG-driven musculoskeletal model improves the human-robot synchronization," *IEEE Trans. Ind. Informat.*, vol. 15, no. 2, pp. 1211–1218, Feb. 2019.
[21] K. E. Gordon and D. P. Ferris, "Learning to walk with a robotic ankle exoskeleton," *J. Biomech.*, vol. 40, no. 12, pp. 2636–2644, 2007.
[22] R. W. Jackson and S. H. Collins, "An experimental comparison of the relative benefits of work and torque assistance in ankle exoskeletons," *J. Appl. Physiol.*, vol. 119, pp. 541–557, 2015.
[23] J. Zhang, C. C. Cheah, and S. H. Collins, "Experimental comparison of torque control methods on an ankle exoskeleton during human walking," in *Proc. IEEE Int. Conf. Robot. Autom.*, 2015, pp. 5584–5589.
[24] J. Zhang, C. C. Cheah, and S. H. Collins, "Torque control in legged locomotion," in *Bioinspired Legged Locomotion: Models, Concepts, Control and Application*. Oxford, U.K.: Butterworth-Heinemann, 2017, pp. 375–428.
[25] K. A. Witte, J. Zhang, R. W. Jackson, and S. H. Collins, "Design of two lightweight, high-bandwidth torque-controlled ankle exoskeletons," in *Proc. IEEE Int. Conf. Robot. Autom.*, 2015, pp. 1223–1228.
[26] J. F. Veneman, R. Ekkelenkamp, R. Kruidhof, F. C. T. van der Helm, and H. van der Kooij, "Design of a series elastic- and bowden cable-based actuation system for use as torque-actuator in exoskeleton-type training," in *Proc. 9th IEEE Int. Conf. Rehabil. Robot.*, 2005, pp. 496–499.
[27] P. G. Jung, G. Lim, S. Kim, and K. Kong, "A survey of iterative learning control," *J. IEEE Control Syst.*, vol. 26, no. 3, pp. 96–114, Jun. 2006.
[28] Y. L. Han and X. S. Wang, "The biomechanical study of lower limb during human walking," *Sci. China Technol. Sci.*, vol. 54, no. 4, pp. 983–991, 2011.
[29] M. W. Whittle, Ed., *An Introduction to Gait Analysis*, 4th ed. Oxford, U.K.: Butterworth-Heinemann, 2004.
[30] H. J. Hermens, B. Freriks, C. D. Klug, and G. Rau, "Development of recommendations for SEMG sensors and sensor placement procedures," *J. Electromyography Kinesiol.*, vol. 10, no. 5, pp. 361–374, 2000.
[31] A. Phinyomark, C. Limsakul, and P. Phukpattaranont, "EMG feature extraction for tolerance of 50 Hz interference," in *Proc. 4th PSU-UNS Int. Conf. Eng. Technol.*, 2009, pp. 289–293.
[32] R. Boostani and M. H. Moradi, "Evaluation of the forearm EMG signal features for the control of a prosthetic hand," *J. Physiol. Meas.*, vol. 24, no. 2, pp. 309–319, 2003.
[33] F. C. Anderson and M. G. Pandy, "Individual muscle contributions to support in normal walking," *Gait Posture*, vol. 17, pp. 159–169, 2003.

Wei Wang received the B.E. degree in computer science and technology from Southwest Jiaotong University, Chengdu, China, in 2012, and the M.S. degree in pattern recognition and intelligent systems from Sichuan University, Chengdu, in 2016. He is currently working toward the Ph.D. degree in control science and engineering with the Institute of Robotics and Automatic Information System, Nankai University, Tianjin, China.

His research interests include biomechanics and lower-limb exoskeleton control and optimization.

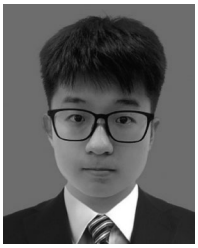

Jianyu Chen received the B.E. degree in automation from the Nanjing University of Aeronautics and Astronautics, Nanjing, China, in 2019. He is currently working toward the Ph.D. degree in control science and engineering with the Institute of Robotics and Automatic Information System, Nankai University, Tianjin, China.

His research interests include wearable assistive robots, control theory, and lower-limb exoskeleton control and optimization.

Yandong Ji is working toward the Undergraduate degree in intelligent science and technology with the College of Artificial Intelligence, Nankai University, Tianjin, China.

His research interests include wearable assistive robots, deep reinforcement learning, and automatic vehicles.

Wei Jin is working toward the Undergraduate degree in intelligent science and technology with the College of Artificial Intelligence, Nankai University, Tianjin, China.

His research interests include wearable assistive robots and medical robots.

Jingtai Liu (Member, IEEE) received the B.E. and M.E. degrees in automation from Tianjin University, Tianjin, China, in 1983 and 1986, respectively, and the Ph.D. degree in robotics from Nankai University, Tianjin, in 1998.

In 1986, he joined Nankai University, where he is currently a Professor of Service Robots with the College of Artificial Intelligence, Nankai Univerisity, Tianjin, China. His research interests include service robots, coexisting–cooperative–cognitive robotics, and artificial intelligence.

Juanjuan Zhang received the B.E. degree in electrical and electronic engineering from Nanyang Technological University, Singapore, in 2007, and the M.S. and Ph.D. degrees in mechanical engineering from Carnegie Mellon University, Pittsburgh, PA, USA, in 2016.

In 2017, she joined Nankai University, where she is currently an Associate Professor of Physical Human-Robot Interaction Control with the College of Artificial Intelligence, Tianjin, China. Her research interests include control theory, medical robots, biomechanics, and lower-limb exoskeleton control and optimization.